

# Peak Laser Intensity – Nonideal Vacuum Role

Dana Dumitriu

27 mai 2021

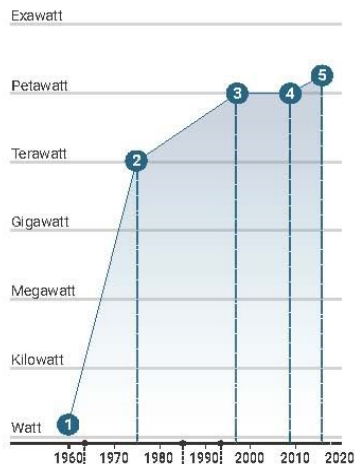




FIG. 8. World map of laser with peak power 1 PW.

## Powering up

Researchers at Lawrence Livermore National Laboratory (LLNL) in Livermore, California, set early power records by amplifying energies in mammoth machines. But a room-size laser in Shanghai, China, now holds the record, after squeezing modest energies into extremely short bursts. Three important techniques have propelled lasers to high powers.



### 1 First laser

Theodore Maiman coaxed laser light from a 2-centimeter-long ruby crystal pumped by photographic flash lamps.



### 2 Janus (LLNL)

The two-beam laser amplified 100-picosecond pulses to 100 joules of energy to create the first terawatt shot.



### 3 Nova (LLNL)

Pulses from the Nova laser were shortened using CPA to achieve the first petawatt.



### 4 National Ignition Facility (LLNL)

Shots focus 192 high-energy pulses on a target to induce fusion. Because the pulses are long, their power does not exceed a petawatt.

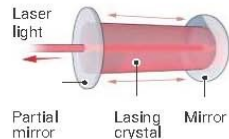


### 5 Shanghai Superintense Ultrafast Laser Facility

By squeezing laser pulses to just tens of femtoseconds, the laboratory achieved record powers with tabletop systems.

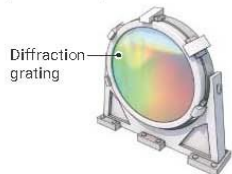
### Mode locking

Although very pure, laser light is emitted over a range of wave lengths, or modes, that resonate in cavities like guitar strings. These modes can be made to constructively interfere for an intense burst tens of femtoseconds long.



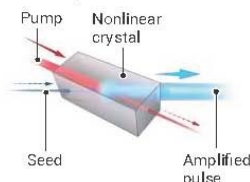
### Chirped-pulse amplification (CPA)

Intense pulses can damage amplifiers. CPA avoids that by stretching a laser pulse with diffraction gratings. After safe amplification, the pulse is compressed.

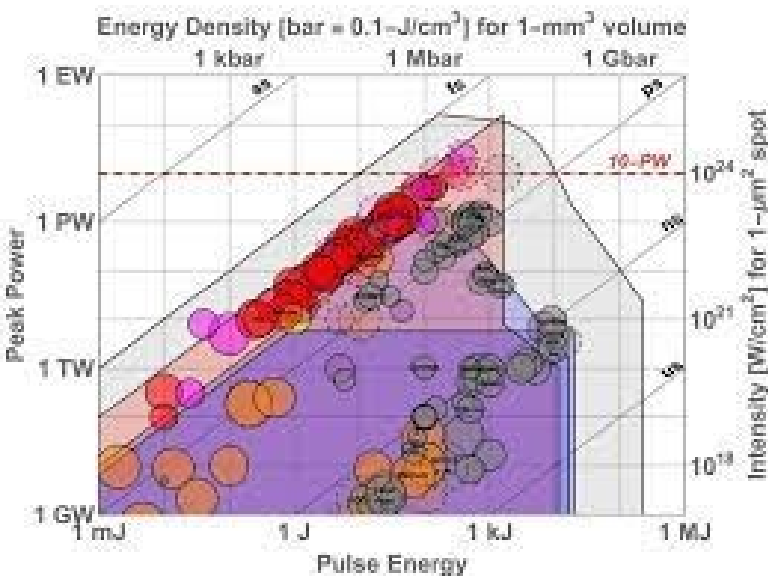


### Optical parametric amplification

A high-energy pump beam can amplify a stretched seed pulse within a nonlinear crystal that can be made large to withstand intense inputs.

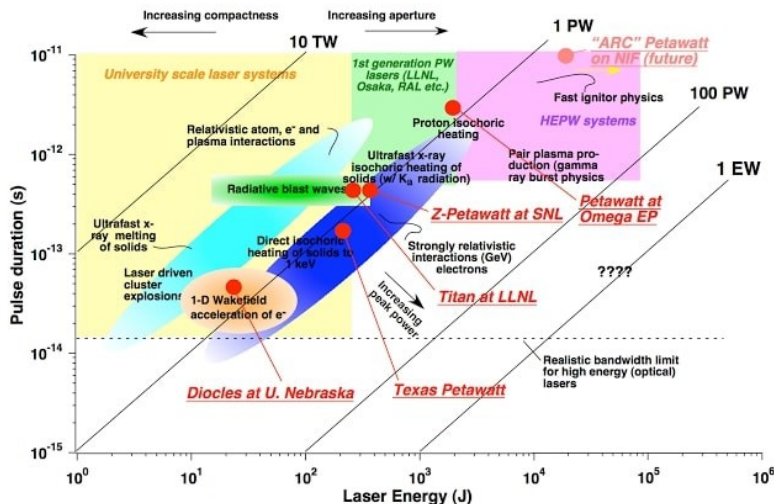


C. BICKEL/SCIENCE

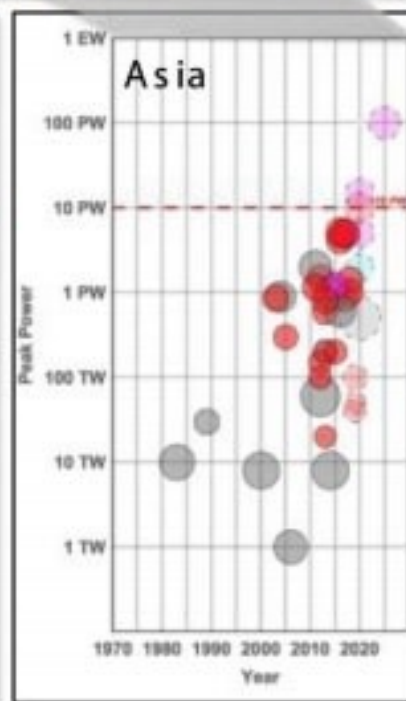
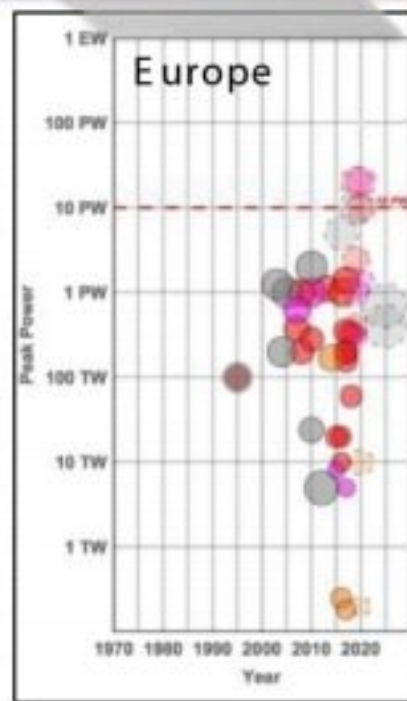
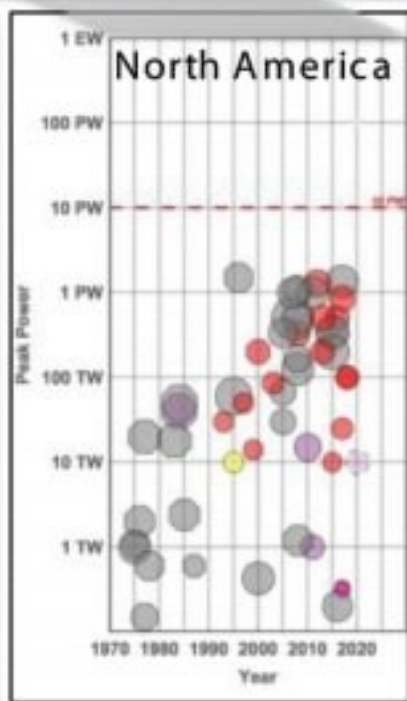
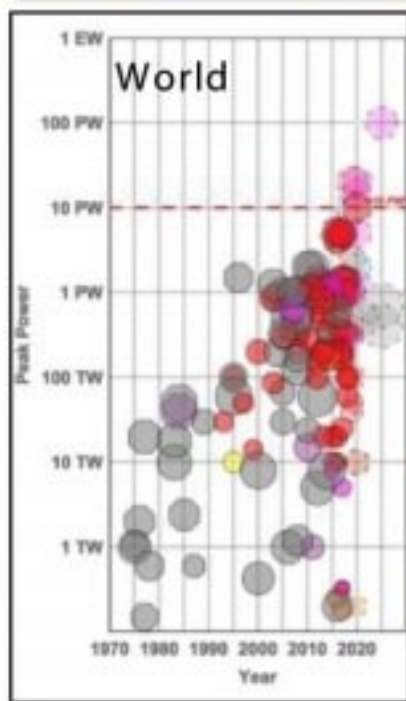


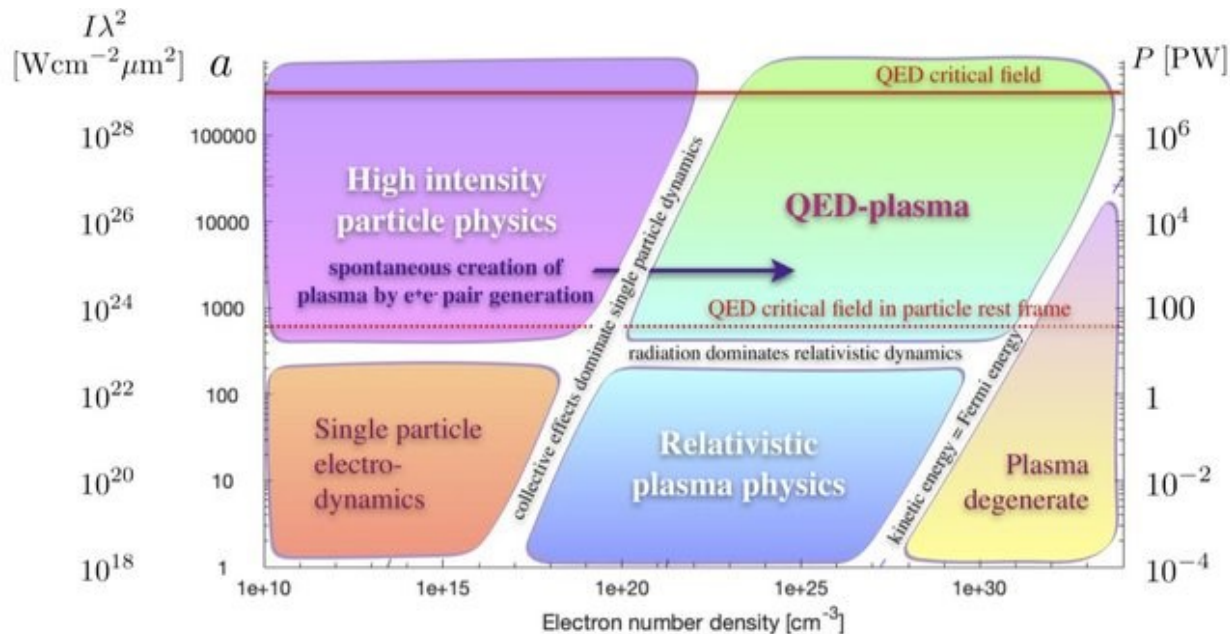
The current high-energy/high-power lasers globally (those that are operational represented by circles with continuous borders; those under construction represented by circles with dashed borders; or those that are decommissioned represented by octagons). The diameter of the symbol is logarithmically proportional to laser pulse energy and the colour indicates the laser media used in the final amplifiers: Ti:sapphire (red), Nd:glass (grey), Yb:X (orange), Cr:X (yellow), optical parametric amplification (purple-blue), or gas (pink)

## Petawatt lasers of differing specifications are needed to access a wide variety of science applications



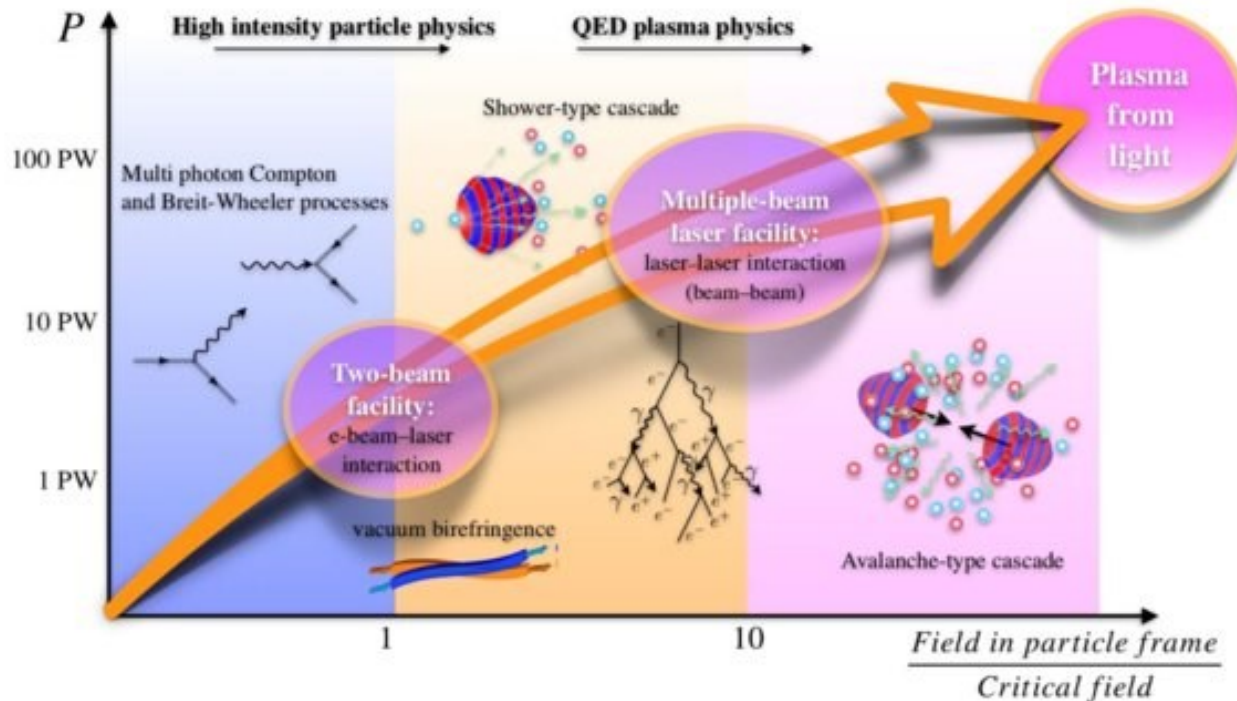
*Petawatt and exawatt class lasers worldwide*



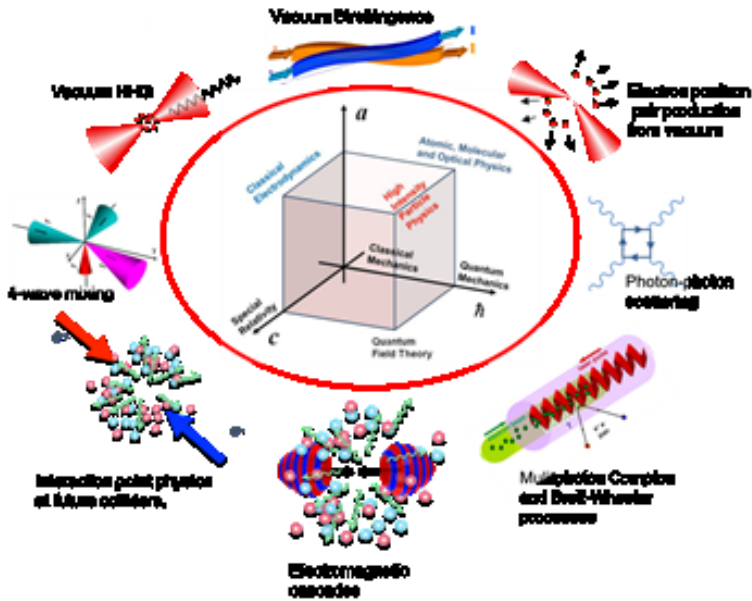


Different regimes of strong field physics as a function of plasma density and laser intensity (left scales) / laser power (right scale).

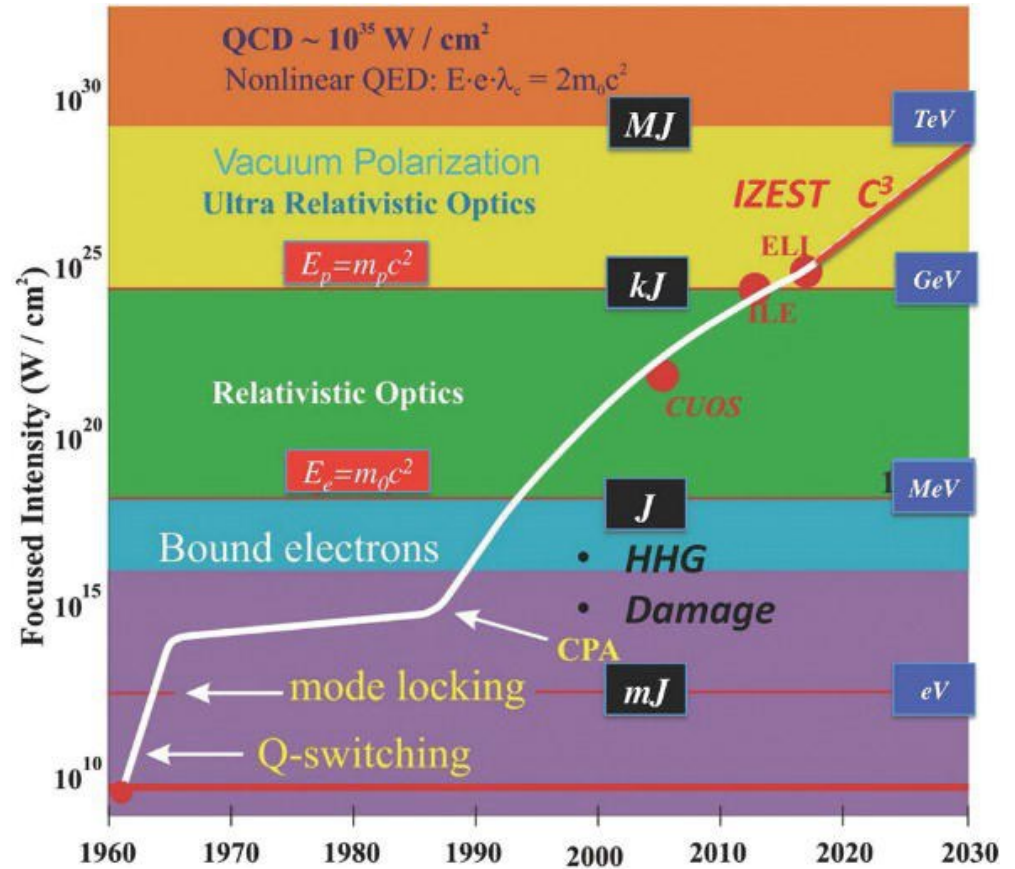
*Timeline of the QED-plasma studies envisioned as a two-stage process with a facility at intermediate laser intensities for the study of fundamental strong-field QED processes, and a multi-beam facility at the highest laser intensities to study the interplay between collective plasma effects and strong field quantum processes.*



# Strong Field Quantum Electrodynamics with high power lasers and particle beams



*The cube of theories, illustrating the relation of Strong Field QED to Quantum Mechanics, Special Relativity, and Quantum Field Theory, as well as typical process happening in strong electromagnetic fields.*



## Peak laser intensities for specific Nd:glass-based lasers

- the Vulcan PW in the UK at  $1 \times 10^{21}$  W/cm<sup>2</sup> (2004);
- the Ti:sapphire based HERCULES laser at the University of Michigan, USA at  $1 \times 10^{22}$  W/cm<sup>2</sup> (2004)
- J-KAREN-P in Japan at  $1 \times 10^{22}$  W/cm<sup>2</sup> (2018)
- record intensity of  $5.5 \times 10^{22}$  W/cm<sup>2</sup> was demonstrated at the CoReLS laser (2019)
- Even the highest-peak-power laser systems (10 PW and beyond) proposed or already in commissioning make no exception to this trend and largely predict intensities of only up to  $10^{23}$  W/cm<sup>2</sup> (notably ELI, EP-OPAL , SULF and SEL).

- At the moment, femtosecond lasers based on the chirped pulse amplification (CPA) technique are regarded as the most reliable approach to realize the highest peak power.
  - After being amplified, compressed, and focused, the peak laser intensity can reach up to  $10^{22}$ – $10^{23}$  W/cm<sup>2</sup>. The 10 PW-class laser facilities, such as ELI, Apollo, Vulcan and SULF aim at boosting the focused intensity by another tenfold.
- 
- Ambitious plans of 100 PW-class have been proposed worldwide, where the peak intensities of  $10^{25}$  W/cm<sup>2</sup> are anticipated. Furthermore, efforts have also been paid in exploring new mechanisms to generate exawatt–zettawatt lasers. At such extreme light intensities, particle acceleration towards 10–100 GeV for leptons and 0.1–10 GeV/nucleon for ions is to be expected.
  - Nuclear physics as well as lab astrophysics will also benefit from these extreme laser sources. Laser–plasma interaction at such intensities enters a new regime where photon emission and radiation reaction become significant and strong-field quantum electrodynamics (SF-QED) is necessary to account for the quantum effects.

- While high-power lasers are under fast development, a central question regarding the ultimate laser intensities researchers can build arises. Basically, the upper limitation for laser intensity in an ideal vacuum condition is considered as the Schwinger field

$$E_s = 2\pi m_e^2 c^3 / eh \sim 1.32 \times 10^{18} \text{ V/m}$$

- The QED theory predicts that laser pulses of  $10^{29} \text{ W/cm}^2$  can provide such field strength in several ways (tight focusing or coherent combining or others), such that they can transfer a large number of virtual particle pairs to real particles. Meanwhile, the generated electron–positron pairs further lose their energies by radiating gamma photons. The laser energy is thus rapidly drained in vacuum.
- Studies have shown that ***even a single pair produced in vacuum by a laser field can lead to rapid depletion of laser energy***, i.e., the maximum light intensity is much smaller than  $10^{29} \text{ W/cm}^2$  in vacuum. It points out that full depletion appears when the energy of generated pairs and photons is equivalent to the energy stored in the pulse, at  $E \sim 6.6\alpha E_s \sim 0.05E_s$   
(corresponding to  $5 \times 10^{26} \text{ W/cm}^2$  for laser wavelength  $\lambda = 800 \text{ nm}$ ).

## *The upper limit*

- The upper limit of the laser field strength in a perfect vacuum is usually considered as the Schwinger field, corresponding to  $\sim 10^{29}$  W/cm<sup>2</sup>.
- This limit can be investigated under realistic nonideal vacuum conditions and find that intensity suppression appears starting from  $10^{25}$  W/cm<sup>2</sup>, showing an upper threshold at  $10^{26}$  W/cm<sup>2</sup>, even if the residual electron density in chamber surpasses  $10^9$  cm<sup>-3</sup> → because the presence of residual electrons triggers the avalanche of quantum electrodynamics cascade that creates many electron and positron pairs.
- The leptons are further trapped within the driving laser field due to radiation reaction, which significantly depletes the laser energy.
- The relationship between the attainable intensity and the vacuum level can be estimated using particle-in-cell simulations tools and theoretical analysis. The results answer a critical problem on the achievable light intensity based on present vacuum conditions and provide a guideline for future hundreds of petawatt class laser development.

- In reality, it is impossible to build a perfect vacuum environment for experiments. Typically, the vacuum electron density in a chamber suitable for PW-class lasers is about  $10^{11} \text{ cm}^{-3}$ , provided by ordinary pumping technique (e.g.,  $10^{-3} \text{ Pa}$  for SULF). For laser power above 100 PW, the chamber volume is enlarged by more than tenfold, posing a great challenge to the pump. Another potential drawback is the existence of electrons extracted from optical components (focusing mirror, plasma mirror, etc.) by the passing laser fields.
- These residual electrons could serve as seeds to trigger the QED processes when the laser field surpasses a certain threshold.
- Specifically, during the laser–electron interaction, nonlinear Compton scattering following  $\mathbf{e} + n\omega \rightarrow \mathbf{e} + \gamma$  will occur, where electrons absorb multiple laser photons and emit high energy  $\gamma$  photons. The radiated  $\gamma$  photons further interact with the strong laser field, generating  $\mathbf{e}^- \mathbf{e}^+$  pairs via the nonlinear Breit–Wheeler process  $\gamma + n\omega \rightarrow \mathbf{e}^+ + \mathbf{e}^-$ . These two reaction channels build up positive feedback, i.e., the amount of the pairs and  $\gamma$  photons will be avalanche-like amplified and deplete the laser significantly, known as the QED cascade. It can be triggered for a single pulse with intensity  $> 10^{25} \text{ W/cm}^2$  or two colliding pulses with intensity  $> 10^{23} \text{ W/cm}^2$ . For more realistic consideration, the depletion is a dynamic process where the laser intensity gradually decreases during the development of a QED cascade, which changes the rate of photon emission and pair production and the later would again deplete the laser energy.

PIC – Particle In Cell - simulations were performed by including the QED models responsible for the two major reaction channels. **Both the simulation and the theoretical model show that the attainable peak intensity depends on the vacuum.**

At electron density about  $10^9 \text{ cm}^{-3}$ , notable energy drain emerges from  $10^{25} \text{ W/cm}^2$  and the upper limit of the laser intensity is modified to  $\sim 10^{26} \text{ W/cm}^2$ .

Two-dimensional (2D) PIC simulations using the code VLPL (Virtual Laser Plasma Lab) was used. It has implemented a **local constant cross-field approximation** (LCFA), QED–Monte Carlo model accounting for nonlinear Compton scattering and Breit–Wheeler processes.

The peak laser amplitude  $a$  is varied from 1500 to 20000, while the vacuum electron density  $n_e$  is tuned between  $10^{11}$  and  $10^{15} \text{ cm}^{-3}$

---

Under LCFA, the newly generated particles gain energies from the parent particles rather than directly from the laser photons. The latter transfer their energies when accelerating the leptons. In our simulations, laser propagates from the left side of a moving simulation window along the  $x$  direction. The window size is  $40 \mu\text{m} (x) \times 80 \mu\text{m} (y)$  resolved by  $4000 \text{ cells} \times 1000 \text{ cells}$ . We set two macroparticles for electrons and protons in each cell. The laser beam is linearly polarized along the  $y$  axis [ $E_L = E_G \cos(\omega t - kx)e_y, B_L = E_G \cos(\omega t - kx)e_z$ ], following a Gaussian profile  $E_G = [aw_0/w(x)] \cos^2[\pi(t - t_f)/2\tau_0] \times \exp[-r^2/w^2(x)]$  focused at  $x_f = 240 \mu\text{m}$  with normalized peak amplitude  $a = eE/m\omega c$  (the corresponding peak intensity  $I_{\text{peak}} = (a^2/\lambda^2) \times 1.38 \times 10^{18} \text{ W/cm}^2$ , with wavelength  $\lambda$  in  $\mu\text{m}$ , where  $m$  is the mass of electron,  $c$  is the velocity of light in vacuum,  $\omega$  is the laser frequency, and  $k$  is the laser wave vector.

---

Another phenomenon limiting the achievable laser intensity is known as radiation-reaction trapping (RRT) in travelling laser field, where the recoiling force of photon emission offsets the pondermotive force, leading to anomalous trapping of leptons in the most intense part of the laser field.

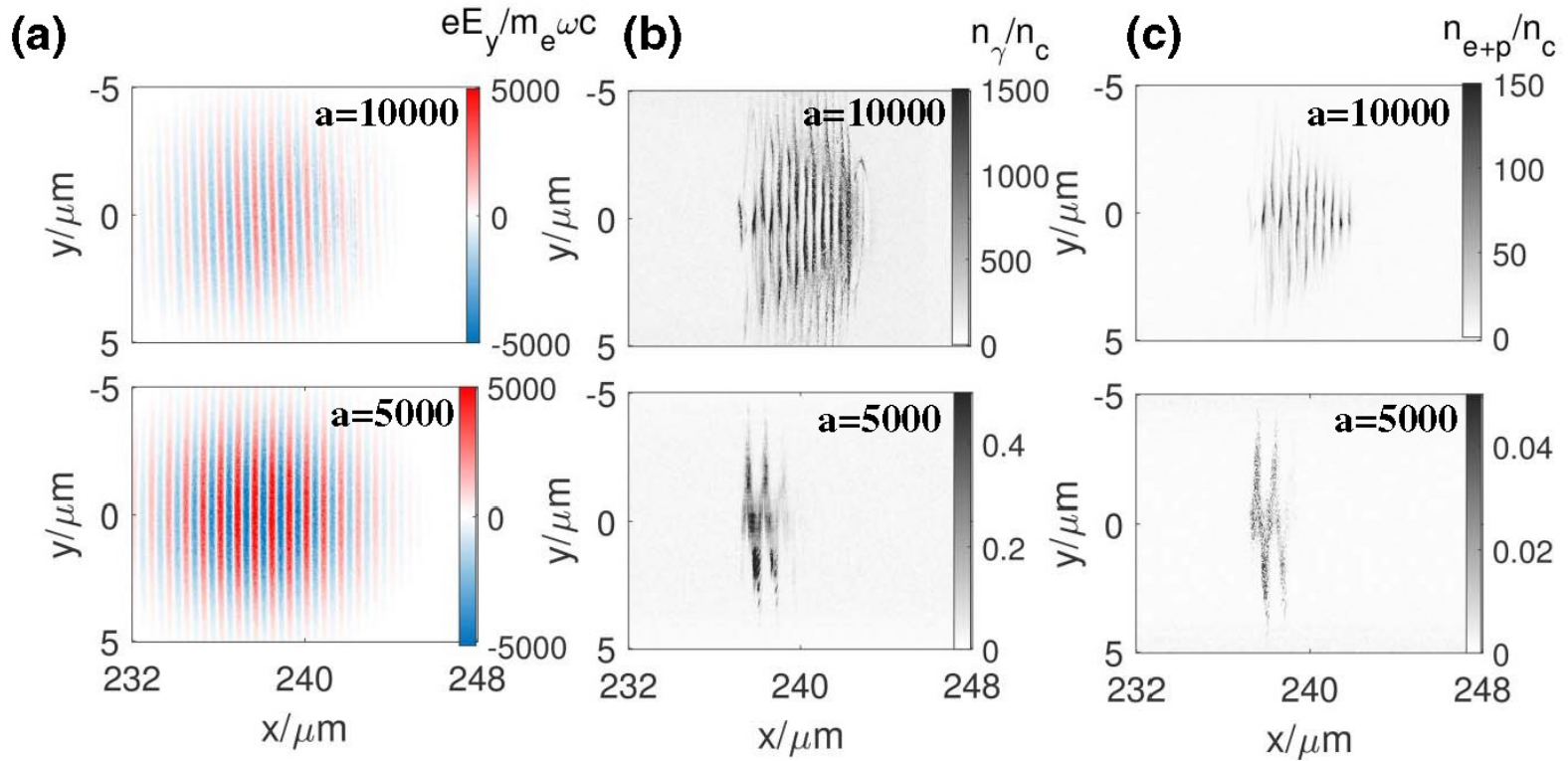


**Fig. 1.** Distributions of (a) laser electric fields  $E_y$  (b)  $\gamma$  photons density  $n_\gamma$  as well as (c) electron–positron density  $n_{e+p}$  at  $t_f = 300T_0$  and  $n_{e0} = 10^{11} \text{ cm}^{-3}$  for  $a = 10000$  (top panel) and  $a = 5000$  case (bottom panel), respectively. The  $E_y$  is normalized by  $m_e \omega c / e$ , while densities are normalized by critical density  $n_c$ .

*The peak laser field amplitude is well preserved for  $a=5000$ , Fig.1(a). However, it declines to be less than 3000 for the other one.*

*The remarkable difference indicates that the attainable light intensity at  $n_{e0} = 10^{11} \text{ cm}^{-3}$  is subject to strong restrictions, and the upper limit appears at  $a=10,000$ .*

*The density distributions of electron–positron pairs  $n_{e+p}$  and  $\gamma$  photons  $n_\gamma$  are shown in Figs. 1(b) and 1(c), where both are about 3 orders of magnitude higher for the  $a 10,000$  case. The density profile shows distinctive patterns between the two cases. We notice that at a 10,000, high density bunches appear all along the laser beam, while at a 5000, density peaks are only seen in the vicinity of highest laser intensity. This is because QED cascade is triggered at the rising edge of the laser pulse for the former such that a large number of electrons and positrons pairs are created at an earlier moment*

A theory that describes the evolution of particle numbers from the QED cascade and give an evaluation for laser energy depletion consider the  $\gamma$  photon and electron–positron pair generation rates satisfying the expression:

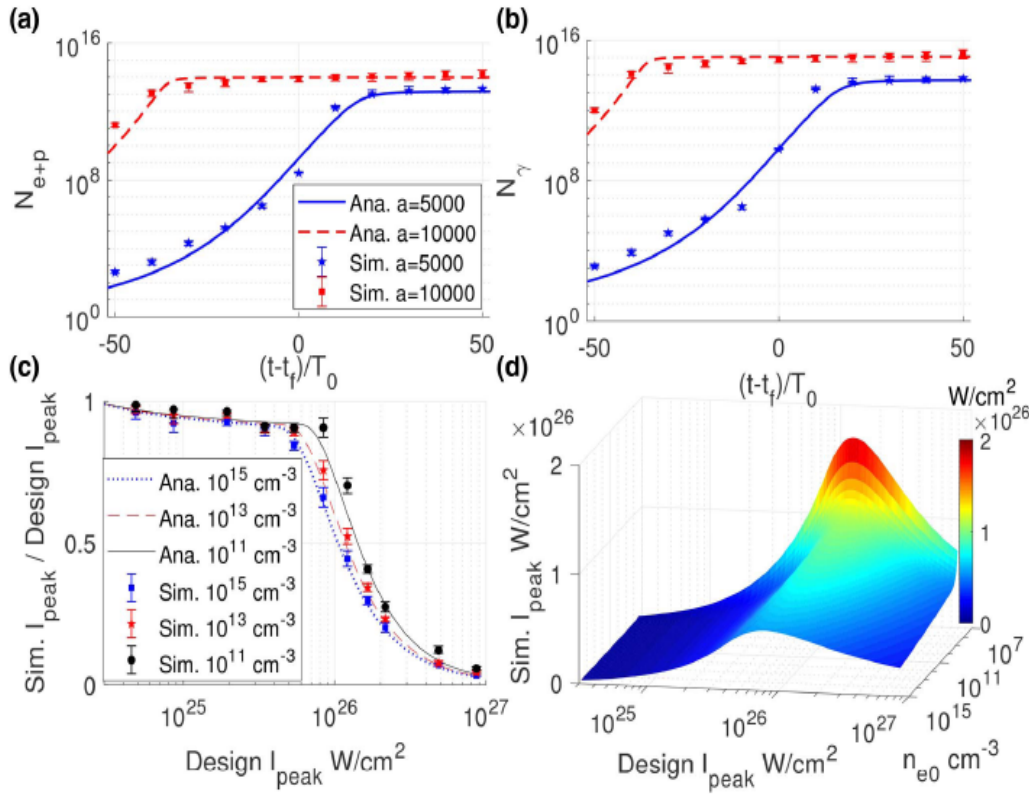
$$\frac{dN_{e+p}}{dt} = 2\Gamma_e N_\gamma,$$

$$\frac{dN_\gamma}{dt} = \Gamma_\gamma N_{e+p} - \Gamma_e N_\gamma,$$

where  $\Gamma_e$  and  $N_{e+p}$  are the generated rate coefficient of electron–positron pairs and number of their total particles, correspondingly;  $\Gamma_\gamma$  and  $N_\gamma$  are the coefficient and number of  $\gamma$  photons, respectively. The generation rate of cascade processes is determined by the QED parameter

$$\chi_i = |(F_{uv} \hat{P}_i^v)|^{1/2} / E_s m_e c \quad (i = \pm e \text{ or } \gamma)$$

where  $F_{uv}$  is the EM field tensor and  $P_i^v$  is the particle's four-momentum



The evolution of  $N_{e+p}$  and  $N_{\gamma}$  based on the above analytical model is given in Figs. 3(a) and 3(b), together with the results collected from PIC simulations. The numbers of both electron-positron pairs and gamma photons undergo exponential growth when the laser interacts with residual electrons, owing to the avalanche-like cascade. When sufficient laser energy is drained, the light intensity declines, and the number of created particles saturates. The above trends are reproduced by the theoretical model.

The peak intensity during focusing processes is measured from PIC simulations and compared to the analytical model. The ratio between the simulated peak intensity and the designed intensity decreases sharply when approaching  $10^{26} \text{ W/cm}^2$  for density from  $10^{11}$  to  $10^{15} \text{ cm}^{-3}$ , corresponding to the energy depletion threshold, Fig3c.

Fig. 3(d), when the designed light intensity surpasses the threshold, the attainable one is restricted to  $10^{26} \text{ W/cm}^2$  for vacuum down to  $10^9 \text{ cm}^{-3}$  according to our theoretical model, exhibiting a clear ceiling. The attainable intensity reaches  $2 \times 10^{26} \text{ W/cm}^2$  for vacuum  $\sim 10^8 \text{ cm}^{-3}$ . It should be noted that at even lower electron densities ( $< 10^7 \text{ cm}^{-3}$ ), the average electron number in the focusing area is less than 1. The cascading effect only occurs when the seeding particle sits in the focal region. In this case, one may not be able to give a definite threshold.

**Fig. 3.** (a)  $N_{e+p}$  and (b)  $N_{\gamma}$  evolution for  $a = 5000$  (blue solid and pentagrams) and  $a = 10,000$  (red dashed and squares) obtained from simulation (symbols) and theoretical analysis (lines); (c) ratio between the measured peak intensity in simulations and the designed one as a function of designed peak intensity under electron densities of  $n_{e0} = 10^{15} \text{ cm}^{-3}$  (blue dotted and squares),  $10^{13} \text{ cm}^{-3}$  (red dashed and pentagrams),  $10^{11} \text{ cm}^{-3}$  (black solid and circles). The symbols are results measured from simulation while lines are from the theoretical model. All symbols represent average values for ten simulation cases with different random seeds, while the error bars represent peak intensity quantile of 95% and 5% (error bar gives a confidence interval of 90%), separately. (d) The theoretical prediction of peak intensity distributions as a function of the designed peak intensity and  $n_{e0}$  (from  $6 \times 10^7$  to  $10^{15} \text{ cm}^{-3}$ ).

# Concluzii

- *Intensitatea maxima care poate fi obtinuta pentru un fascicul laser depinde de conditiile de vacuum*
- *Cascadele QED de tip avalansa si RRT (Radiation Reaction Trapping) influenteaza puternic si limiteaza maximul intensitatii laserului din cauza electronilor reziduali din calea pulsurilor laser*
- *Simularile autorilor YITONG WU, LIANGLIANG JI, AND RUXIN LI, Vol. 9, No. 4 / April 2021 / Photonics Research sugereaza ca intensitatea peak-ului nu mai creste incepand de la  $\sim 10^{25} \text{W/cm}^2$  si ca o limita maxima de  $10^{26} \text{W/cm}^2$  se atinge pentru o densitate a electronilor in vid de  $10^9 \text{cm}^{-3}$*

## Further Reading

*Strong field physics pursued with petawatt lasers,*

Vishwa Bandhu Pathak, Seong Ku Lee, Ki Hong Pae, Calin Ioan Hojbota, Chul Min Kim and Chang Hee Nam, AAPPS Bulletin (2021) 31:4

<https://doi.org/10.1007/s43673-021-00004-5>

*Quantum electrodynamics experiments with colliding petawatt laser pulses*

C. E. Turcu, B. Shen, D. Neely, G. Sarri, K. A. Tanaka, P. McKenna, S. P. D. Mangles, T.-P. Yu, W. Luo, X.-L. Zhu, and Y. Yin  
High Power Laser Science and Engineering, (2019), Vol. 7, e10, 8 pages.

*Polarized QED cascades*

Daniel Seip, Christopher P Ridgers, Dario Del Sorbo and Alec G R. Thomas  
New J. Phys. **23** (2021) 053025

*Towards realistic simulations of QED cascades: Non-ideal laser and electron seeding effects*

Archana Sampath, and Matteo Tamburini

Phys. Plasmas **25**, 083104 (2018); <https://doi.org/10.1063/1.5022640>

*QED cascade with 10 PW-class lasers*

Martin Jirka 1,2, Ondrej Klimo 1,2, Marija Vranic 3, Stefan Weber 1 & Georg Korn 1

[www.nature.com/scientificreports](http://www.nature.com/scientificreports)

[www.nature.com/scientificreports](http://www.nature.com/scientificreports), published online 10 November 2017

*Multumesc !*